JOURNAL OF MATERIALS SCIENCE **40** (2005) 2295–2300

Wetting and spreading of liquid metals on ZrB_2-based ceramics

M. L. MUOLO, E. FERRERA, A. PASSERONE
IENI-GE, CNR, Via De Marini 6, 16149-Genoa, Italy
E-mail: ml.muolo@ge.ieni.cnr.it

The possibility to exploit commercially the peculiar characteristics of refractory metallic and ceramic materials and in particular of Zirconium diboride ceramics—a class of promising materials for high temperature applications—often depends to a great extent on the ability to join different ceramics one to the other or to special metallic alloys. As the behaviour of a metal-ceramic joint is ruled by the chemical and the physical properties of the interface, the knowledge of wettability, interfacial tensions and interfacial reactions is mandatory to understand what happens at the liquid metal-ceramic interface during joining processes.

In the framework of an extensive study aimed at evaluating the wettability and the interfacial characteristics of different metal-ceramic systems, the behaviour of ZrB_2 in contact with liquid Ag and its alloys (Cu, Ti, Zr, Hf) has been studied. ZrB_2 pure, with different sintering aids or "alloyed" with other ceramic materials (SiC, Si_3N_4), have been used.

The wetting and spreading experiments have been performed by the sessile drop technique under controlled atmospheres. The wetting and spreading characteristics and the interfacial reactions are discussed as a function of time, compositions of the ceramic and of the alloy involved. The interfacial morphologies, analysed by SEM and EDS, show the presence of regular interfaces and adsorption layers and of different bulk phases which are interpreted in terms of the relevant phase-diagrams.

1. Introduction

The increasing demand for high temperature materials, able to survive in extremely severe conditions, where not only temperature, but also wear, corrosion and mechanical loads represent the working conditions, has led to identify new classes of compounds ranging from oxides, to carbides, nitrides and borides [1]. They can be used in the form of coatings to protect the underlying structural metallic alloys, or as bulk, thick components, where high temperatures and high heat fluxes are involved. This is particularly the case in combustion chambers of turbines or when special Thermal Protection Systems have to be designed to protect the outer structure of space vehicles in the atmospheric re-entry phase [2–5]. Indeed, to reduce the thermal exchange between the atmosphere and the vehicle structures during the re-entry operations, an alternative to ceramic coatings is to improve the thickness of the protective layer using bulk ceramics.

In this latter case, ceramic materials should be chosen with high melting point, high oxidation resistance, good thermal shock resistance, low vapour pressure, good creep properties and well suited (metal-ceramic) thermal expansion coefficients.

Recent calculations [6, 7], confirmed by ad-hoc experimental tests, based on exposure profiles coherent with the experimental mission profiles, have shown that, under heavy thermal conditions, (surface temperature exceeding 2000 K, heat fluxes of the order of 1 MW/m^2), a good thermal insulation can be obtained only with thick ceramic layers. This configuration calls for ad-hoc procedures to fasten these layers to the aircraft metallic structure: among the different possibilities, the utilisation of brazing techniques, involving the presence of a transient layer of liquid filler alloy, should be taken into serious consideration. However, the behaviour of metal-ceramic joints is ruled by the chemical and the physical properties of the interface. Thus, the knowledge of wettability, interfacial tensions and interfacial reactions is mandatory to understand what happens at the liquid metal-ceramic interface during the joining processes [8].

This paper presents the results of wetting, spreading and joining of Zirconium Boride ceramics, both pure and modified by sintering aids, by Ag and Cu and their alloys with active metals of the IV group Ti, Zr and Hf. The joining tests have been made with the Ti-6Al-4V alloy. The results will be discussed in terms of interfacial thermodynamic properties (work of adhesion, interfacial tension) and interfacial microstructures.

2. Experimental

2.1. Materials

2.1.1. Ceramics

The sintered ceramic bodies have been prepared by ISTEC-CNR starting from pure ZrB_2 powders or

TABLE I Properties of ZrB_2 samples used in the present work: HV is the Vickers μ hardness with an applied load of 9.81 N, K_{IC} is the fracture toughness measured by (CNB) chevron notched beam method, T is the sintering temperature, ρ is density, % respect to the full density, λ is the thermal expansion coefficient and E is the Young's modulus [9–12]

HV (GPa)	K_{IC}(CNB) (MPa$\sqrt{m}$)	(ZrB_2)	T (K)	ρ (g/cm^3)	(%)	λ 10^{-6}(K) 1073 K	1273 K	1573 K	E (GPa)
8.7 ± 0.4	2.35 ± 0.15	pure	2173	5.28	86.5	7.12	7.32	7.60	346
14.4 ± 0.8	3.4 ± 0.4	+4 wt% Ni	2123	6.05	98	7.49	7.70	7.51	496
13.4 ± 0.6	3.57 ± 0.61	+2.5 wt% Si_3N_4	1973	5.85	98	–	–	–	–
14.6 ± 0.3	–	+20 wt% SiC +4 wt% Si_3 N_4	2143	5.30	98	7.00[a]	7.48[a]	7.43[a]	–

[a]Calculated data.

adding known quantities of Ni and Si_3N_4 as sintering aids to control the processing parameters, the final porosity and consequently to improve the final characteristics of the ceramics, while SiC has been added to improve the mechanical properties [9–12].

The presence of Ni promotes the formation of liquid phases at high temperature ($T \geq 1533$ K) which have two main effects: to favour the powder particle rearrangement and to enhance mass transfer mechanisms that improve sintering.

A further reduction in sintering temperature (1973 K), a great improvement in densification and microstructure have been obtained by adding, to pure zirconium diboride, 2.5 wt% of Si_3N_4.

At the sintering temperature the silicon nitride completely disappears leading to various compounds (BN, t-ZrO_2, $ZrSi_2$, amorphous B-N-O-Si-Zr glass) as confirmed by XRD analysis. The secondary phases are mainly concentrated at grain boundaries and triple points (Table I).

2.1.2. Metals and alloys

Pure Ag and Cu (Marz grade 99.998) have been used, also to form the required alloys with Ti, Zr and Hf (99.9%) by adding, *in situ*, the required amount of the active metal (2.4 at%) to a pre-melted bead of the matrix metal. All additions have been set at the same atomic concentration to allow comparisons to be made. The commercial Ag-Cu-Ti alloy (70-27-3 wt%) (Degussa) has also been used. Joining tests have been made with the commercial (Titalia) Ti-6Al-4V alloy. All materials have been carefully cleaned by mechanical and chemical means just prior to each experiment.

2.2. Wetting tests

Wetting experiments have been performed by the Sessile-Drop technique [13, 14] in a special tubular furnace made up of two concentric, horizontal, alumina tubes, connected to a high vacuum line. Between the tubes an Ar flow is maintained, in order to avoid any diffusion of atmospheric oxygen into the working chamber at high temperature. A vacuum better than 10^{-4} Pa or a controlled atmosphere can be set in the working tube, the oxygen partial pressure being measured by a solid state gauge at the exit of the inner tube. An optical line allows sessile drops in the center of the working chamber to be imaged by a CCD camera. A specifically developed image analysis software (ASTRAView [15, 16]) allows the surface tension, contact angles and other drop's parameters to be computed in real time during the experiments.

All sessile drop experiments and junctions reported here have been made under a controlled flow of Ar + 5%H_2 (flow rate = 50 cm^3/min), at 1323 or 1423 K. The ceramic plates (15 × 15 × 2 mm) and the metal pieces were put in the center of the tube when all the physico-chemical parameters were at equilibrium. The samples, maintained at temperature for 30 min, were cooled down quickly, by pulling them out of the furnace.

A Zr getter has been put around the sample in order to reduce its oxidation. Taking into account the oxygen partial pressure coming from the oxidation of the Zr getter we can estimate a P_{O_2} of the order of 10^{-27} Pa for a dry atmosphere. As a matter of fact, our gas contains 5% H_2 so, taking into account the water equilibrium, our oxygen pressure can locally rise to an average value of 10^{-17} Pa. The average surface roughness of the ceramics, after polishing, was found to be in the order of 0.05 μm. Contact angles are measured with a reproducibility of $\pm 3^\circ$ between the runs. However, the presence, especially for the $(ZrB_2)_{pure}$, of a relevant surface porosity (approx. 10% of the area), can lead to occasional higher uncertainties in the measured contact angles, especially when θ is greater than 130° or smaller than 30°.

The specimens have been characterised by optical and SEM observations and EDS.

2.3. Joining tests

Joining tests have been performed in the same apparatus and experimental conditions used for the wetting tests.

No extra pressure has been applied on the sample. The contact among the solid components has been secured by means of a small stainless steel clip.

An Ag-Zr sheet, 100 μm thick, has been put between ZrB_2-Si_3N_4 ceramic and TiAlV metal plates previously polished to $Ra \cong 0.02$ μm.

The samples, maintained at 1323 K for 30′, have been cooled down at 4 K/min.

3. Results

3.1. Wetting results

Wetting results are reported in Table II and in Figs 1 and 2, while Figs 3 and 4 show the spreading curves of the Ag-Zr alloy on different substrates (Fig. 3) and of

TABLE II Surface tension, contact angles and work of adhesion for Ag-X alloys on pure ZrB_2

Metal/alloy (at%)	σ (mN/m) $T = 1323$ K	σ (mN/m) $T = 1423$ K	θ ($T = 1323$ K) (on ZrB_2 pure)	W_{ad} (mJ/m^2) $T = 1323$ K	$\sigma \cos\theta$ (mN/m) $T = 1323$ K
Ag	913	898	>140°	<213.6	− 699.4
Cu		1272	$>140_{1423K}$	$<300_{1423K}$	− 974.4
$(Ag\text{-}Cu)_{eut}$	981	968	141°	218.6	− 762.4
$(Ag\text{-}Cu)_{eut}$-Ti 2.4	1077	1068	30°	2009.7	932.7
$(Ag\text{-}Cu)_{eut}$-Zr 2.4	1075	1066	52°	1736.8	661.8
Ag-Ti 2.4	931	916	27°	1760.5	829.5
Ag-Zr 2.4	929	914	21°	1796.3	867.3
Ag-Hf 2.4	933	918	$75°_{1323K}$	1174.5	238.9
			$53°_{1423K}$	1470.5	552.5

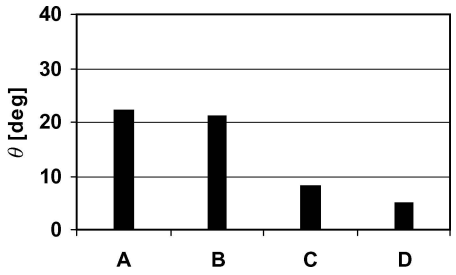

Figure 1 Contact angles of (AgZr) on different substrates: A = (ZrB_2 + Ni), B = (ZrB_2), C = (ZrB_2 + Si_3N_4), D = (ZrB_2 + SiC + Si_3N_4) at T = 1323 K.

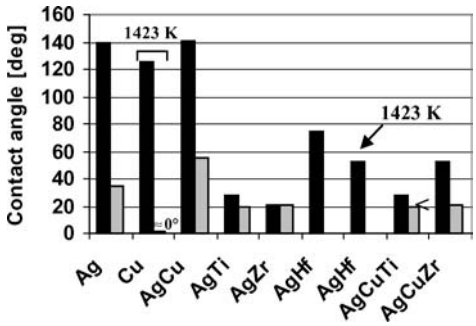

Figure 2 Contact angles of different alloys on ■ ZrB_2 and on □ ZrB_2 + Ni at T = 1323 K (error on $\theta = \pm 2°$).

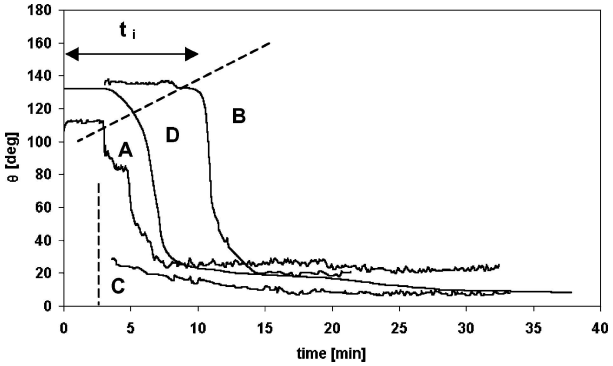

Figure 3 Contact angles of AgZr alloy on different substrates at T = 1323 K; A = (ZrB2+ Ni), B = (ZrB_2), C = (ZrB_2 + Si_3N_4), D = (ZrB_2 + SiC + Si_3N_4) at T = 1323 K.

different alloys on the pure ZrB_2 (Fig. 4). The different spreading curves cannot be superimposed because the initial time does not represent specimens in the same physico-chemical conditions. Indeed, the melting and homogenisation time is not the same in all runs: on the contrary, once the active element is "available" in

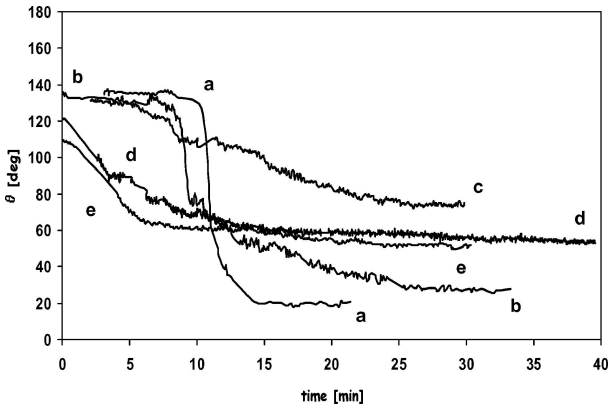

Figure 4 Contact angles of different alloys on ZrB_2 at T = 1323 K; a = AgZr, b = AgTi, c = AgHf, d = AgHf (1423 K), e = AgCuZr.

the liquid alloy, the spreading curves take on their full significance and can be compared to each other.

As shown, $(ZrB_2)_p$ is not wet by the pure metals Ag and Cu (at 1423 K), nor by the eutectic Ag-Cu alloy. A sharp decrease in contact angle is obtained by adding an "active" element, Ti, Zr or Hf, to the molten Ag matrix. However, the extent of this effect is different for the various metals. Zr seems to be the most effective in promoting wettability of the pure boride, while Hf reaches a higher interfacial activity only at temperatures above 1400 K. Both Ti and Zr improve the wetting behaviour of the eutectic Ag-Cu alloy, but to a lesser extent than in the case of the pure Ag.

In order to evaluate the energetics of the interaction phenomena at the experimental temperature, the Work of Adhesion ($W_{ad} = \sigma\ (1 + \cos\theta)$) can be calculated, provided the surface tension σ of the molten phase is known. The pure metals surface tension values are from ref. [17] (Ag, Cu) and from ref. [18] for Ti, Zr and Hf, extrapolated to 1323 and 1423 K. Alloys surface tensions have been computed by a quasi-chemical solution model [19, 20] previously developed. It is easily seen that, as expected, the addition elements tend to rise the liquid alloy surface tension with respect to the matrix, confirming that the relevant phenomenon which promotes wetting is the segregation of the active element to the solid-liquid interface. This is also clearly shown by the high values of the Work of Adhesion obtained for the systems with Ti, Zr and Hf additions.

It is worth reminding that the term ($\sigma \cos\theta$) represents the amount by which the solid surface tension is decreased by the solid-liquid interactions to give the

interfacial tension value ($\sigma_{sv} - \sigma_{sl} = \sigma \cos\theta$). Provided the solid surface tension does not vary in the present case, when going from one liquid alloy to the other (indeed, the same metal matrix is used, the additional elements have very low vapour pressures and the experimental conditions are the same), the values in the last column in Table II clearly show that Zr is much more efficient in adsorbing/reacting at the interface and promoting wetting.

On the other hand, the different sintering aids used to improve both the density of the final ceramic product and to increase their toughness have a relevant effect on their wettability. The beneficial effect of Ni additions to the solid phase can be easily understood taking into account that Ni segregates to the grain boundaries. A more or less continuous Ni network exists at the ceramic surface, which increases its overall metallicity and its wettability by the different alloys. The nearly perfect wetting found with Cu, with respect to the "good" wetting obtained with other alloys, is to be ascribed to the higher experimental temperature (1423 K) which helps decomposing possible NiO layers (at this T the Ni + O = NiO equilibrium oxygen partial pressure is of the order of 10^{-2} Pa, the same in the flowing gas, without getters). A similar beneficial effect has been found with Si_3N_4additions. In this system, complex intergranular phases form during the sintering stage, like the amorphous B-N-O-Si-Zr glass [9, 11], which emerge at the ceramic surface and interact directly with the molten metallic phase. Very good wetting has been obtained with Ag-Zr on ZrB_2 + Si_3N_4 and on ZrB_2 + Si_3N_4 + SiC on which the molten alloy spreads with a fast kinetics covering the entire surface of the sample.

Wetting tests of Ti-Al-V alloy have also been made, using the Ag-Zr alloy at 1323 K. Complete wetting was obtained, with a very fast kinetics, taking place in a few seconds. The wetting alloy has shown a strong tendency to interact at the solid-liquid interface to form solid solutions and a certain degree of Ag intergranular penetration.

3.2. Microstructures

The structures of the solid-liquid interfaces have been studied on vertical sections of the solidified samples by SEM and microanalysis. The metallographic sections of the $(ZrB_2)_{pure}$/Ag-X samples show a sharp interface where no detectable interlayers of reaction products have been found (Figs 5–7). In the metal phase, starting from open voids of the ceramic, microanalysis have identified the Ag-Zr or Ag-Hf intermetallic phases (elongated crystals), according to the phase diagram [21, 22], embedded in a matrix which is essentially formed only of Ag. On the contrary, in the case of the Ag-Ti system, a continuous Ti–rich layer is found at the solid-liquid interface. This layer should have been originated from Ti adsorption more than from interfacial reactions: indeed, the ZrB_2 phase does not present any corrosion or degradation sign. This fact is further confirmed by the specimens used for joining tests, as discussed below.

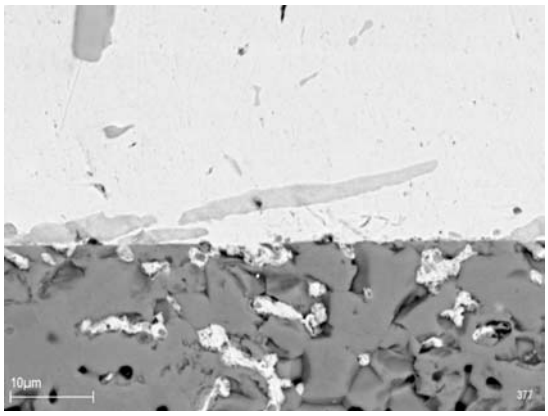

Figure 5 SEM micrograph of Ag-Zr (top)/$(ZrB2)_{pure}$ wetted interface.

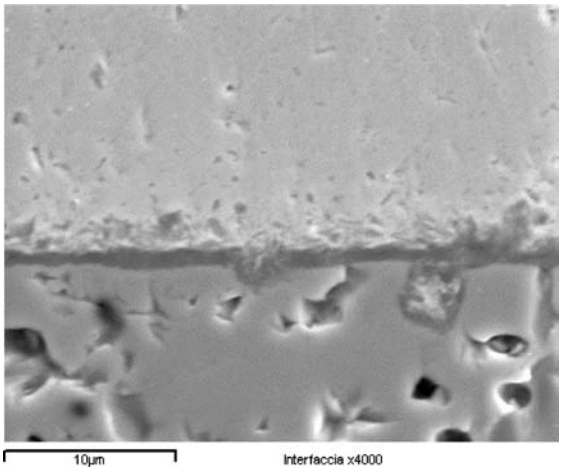

Figure 6 SEM micrograph of Ag-Ti (top)/$(ZrB2)_{pure}$ wetted interface.

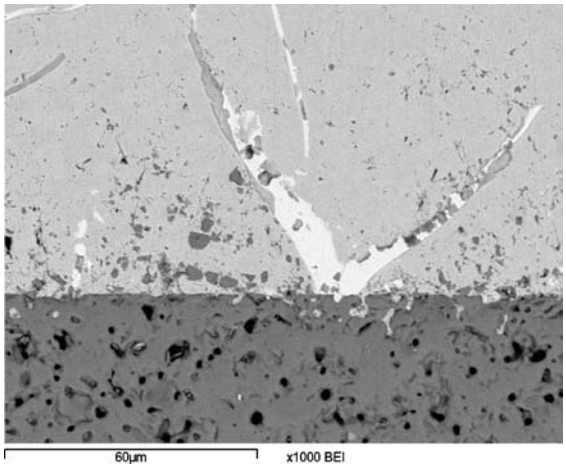

Figure 7 SEM micrograph of Ag-Hf (top)/$(ZrB_2)_{pure}$ wetted interface.

Despite the high density of the ZrB_2 sintered with Ni, the metal-ceramic interface appears very uneven (Fig. 8). Two different layers, grown into the metal, have been put in evidence by SEM. Near the ceramic a dark grey layer, of the order of 10 μm, has a composition rich in Zr (61 wt%), Ni (35 wt%) and poor in Ag (4 wt%). The clear grey zone is thicker and its composition is comparable to the NiZr intermetallic phase (Ni39 wt%-Zr61 wt%). The bulk drop is nearly 100% Ag.

The microstructure of the junction layer presents some peculiarities (Fig. 9). The filler alloy has a

Figure 8 SEM micrograph of Ag-Zr (top)/$(ZrB_2)_N$ wetted interface.

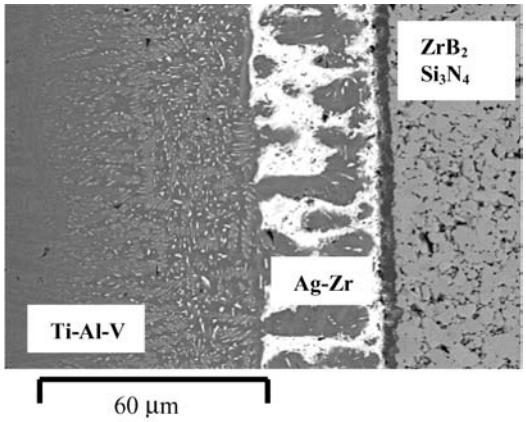

(a)

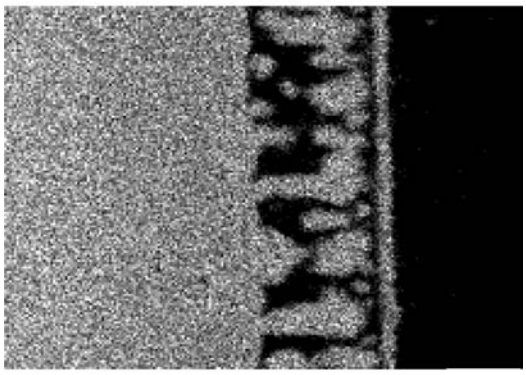

(b)

Figure 9 Cross section of the joined interface: ZrB_2-Si_3N_4/Ag-Zr/Ti-Al-V. (a) SEM-BEI image; (b) Ti map, showing the strong diffusion of Ti from the bulk TiAlV through the Ag-Zr filler alloy up to the ceramic interface.

columnar structure, quite regular, where Ag-rich (dark areas in Fig. 9b) and Ti-rich phases are predominant. It is also possible to single out two different substructures according to the phase diagram and coming from the peritectic reaction of the Ag-Ti system. Ti from TiAlV dissolves into the filler metal and tends to accumulate at the ceramic interface as shown in Fig. 9b, contributing to promote the wetting, as already found in the wetting tests with the Ag-Ti alloy. Silver, on the contrary, diffuses into TiAlV for about 60 μm. No reaction products seem to exist at the interface inside the ceramic phase.

4. Conclusions

Among the different options for joining dissimilar materials, liquid-phase bonding (brazing) is one of the most interesting techniques by which reliable parts can be produced. In order to find the critical parameters governing this process, experiments on the wetting behaviour of the refractory boride ZrB_2, with different additions, and joining tests of this boride with the Ti6Al4V structural alloy have been made.

Different filler alloys have been tested, and optimal results have been obtained with Silver-based alloys with additions of interfacial-active metals of the IV Group Ti, Zr and Hf. All these alloys show low contact angles on the zirconium boride refractory, both sintered pure and with various sintering aids. A common interesting feature, demonstrated by interfacial microstructures and EDS analysis, is that the metal-ceramic interface remains quite sharp after the wetting process, at variance with what happens with the same, or similar alloys with oxidic ceramics (e.g. alumina, zirconia [23–26]) thus allowing better mechanical properties to be obtained in the joining processes. In this respect, the Ag-Zr alloy has shown a great potential as metal braze for the ZrB_2/TiAlV couple.

Acknowledgements

The authors would like to express their appreciation to Drs. Alida Bellosi and Frederic Monteverde for the preparation of ceramic samples in the framework of the ASI-CNR contracts 073/01 and 251/02, to Dr. Claudio Zanotti for the fruitful help and discussions on thermal exchange, and to Mr. Carlo Bottino for SEM and EDS analyses.

References

1. N. B. DAHOTRE, P. KADOLKAR and S. SHAH, *Surf. Inter. Anal.* **31** (2001) 659.
2. K. UPADHYA, J. M. YANG and W. P. HOFFMAN, *Am. Cer. Soc. Bull.* **72** (1997) 51.
3. D. RASKY, J. SALUTE, P. KOLODZIEJ and J. BULL, in 3rd European Workshop Thermal Protection Systems,WPP-141 (ESA Publications, ESTEC, Noordwijk, 1998) p. 363.
4. A. DE ROOIJ, in Materiali per lo spazio: sintesi, metodologie, tecnologie, edited by A. Passerone and M. L. Muolo (Grafiche G. & G. Del Cielo, Genova, 2001) p. 1.
5. G. RAMUSAT, in Materiali per lo spazio: Sintesi, metodologie, tecnologie, edited by A. Passerone and M. L. Muolo (Grafiche G. & G. Del Cielo, Genova, 2001) p. 17.
6. N. BERTOLINO, M. MONAGHEDDU, A. TACCA, P. GIULIANI and C. ZANOTTI, in Hot Structures and Thermal Protection Systems for Space Vehicles, SP-521 (ESA Publication Division, ESTEC, Noordwijk, 2003) p. 155.
7. A. PASSERONE, M. L. MUOLO, L. MORBELLI, E. FERRERA, M. BASSOLI and C. BOTTINO, in "Hot Structures and Thermal Protection Systems for Space Vehicles, SP-521" (ESA Publication Division, ESTEC, Noordwijk, 2003) p. 295.
8. N. EUSTATHOPOULOS, M. G. NICHOLAS and B. DREVET, "Wettability at High Temperature" (Pergamon, Amsterdam, 1999).
9. F. MONTEVERDE and A. BELLOSI, *Scripta Mater.* **46** (2002) 223.
10. A. BELLOSI, F. MONTEVERDE, D. DALLE FABBRICHE and C. MELANDRI, *J. Mater. Proc. & Manuf. Sci.* **9** (2000) 156.

11. F. MONTEVERDE, S. GUICCIARDI and A. BELLOSI, *Mater. Sci. Eng.* **A346** (2003) 310.
12. A. BELLOSI, F. MONTEVERDE and S. GUICCIARDI, *J. Am. Ceram. Soc.* **22** (2002) 279.
13. A. PASSERONE and E. RICCI, in "Drops and Bubbles in Interfacial Research," edited by D. Moebius and R. Miller (Elsevier, Amsterdam, 1998) Vol. 6, p. 475.
14. M. L. MUOLO, E. FERRERA, R. NOVAKOVIC and A. PASSERONE, *Scripta Mater* **48** (2003) 191.
15. L. LIGGIERI and A. PASSERONE, *High Temp. Techn.* **7** (1989) 80.
16. M. VIVIANI, L. LIGGIERI and A. PASSERONE, IENI-CNR Technical Report, CNR, Genoa (2002).
17. J. C. JOUD, N. EUSTATHOPOULOS and P. DESRÉ, *C.R. Acad Sc Paris: Série* F;C, 274, (1972) 549.
18. T. ISHIKAWA, P. F. PARADIS, T. ITAMI and S. YODA, *J. Chem. Phys.* **118** (2003) 7912.
19. R. NOVAKOVIC, E. RICCI, M. L. MUOLO, D. GIURANNO and A. PASSERONE, *Intermetallics* **11** (2003) 1301.
20. R. NOVAKOVIC, M. L. MUOLO and A. PASSERONE, *Surf. Sci*. **549** (2004) 281.
21. T. B. MASSALSKI, "Binary Alloy Phase Diagrams" (Am. Soc. for Metals, Ohio, 1986) Vol. 1, p. 87.
22. H. OKAMOTO, *J. Phase Equil*. **17** (1996) 547.
23. P. KRITSALIS, L. COUDURIER and N. EUSTATHOPOULOS, *J. Mater. Sci.* **26** (1991) 3400.
24. N. IWAMOTO and H. YOKOO, *ibid.* **27** (1992) 441.
25. T. TORVUND, Ø. GRONG, O. M. AKSELSEN and J. H. ULVENSOEN, *Metallurg. Mater. Trans. A* **27A** (1996) 3630.
26. D. SCITI, A. BELLOSI and L. ESPOSITO, *J. Europ. Ceram. Soci.* **21** (2001) 45.

Received 31 March
and accepted 20 October 2004